Sensing-Driven Energy Purchasing in Smart Grid Cyber-Physical System

Chen-Khong Tham, *Member, IEEE*, and Tie Luo

***Abstract*—Distributed and renewable-energy resources are likely to play an important role in the future energy landscape as consumers and enterprise energy users reduce their reliance on the main electricity grid as their source of electricity. Environmental or ambient sensing of parameters such as temperature and humidity, and amount of sunlight and wind, can be used to predict electricity demand from users and supply from renewable sources, respectively. In this paper, we describe a Smart Grid Cyber-Physical System (SG-CPS) comprising sensors that transmit real-time streams of sensed information to predictors of demand and supply of electricity and an optimization-based decision maker that uses these predictions together with real-time grid electricity prices and historical information to determine the quantity and timing of grid electricity purchases throughout the day and night. We investigate two forms of the optimization-based decision maker, one that uses linear programming and another that uses multi-stage stochastic programming. Our results show that sensing-driven predictions combined with the optimization-based purchasing decision maker hosted on the SG-CPS platform can cope well with uncertainties in demand, supply, and electricity prices and make grid electricity purchasing decisions that successfully keep both the occurrence of electricity shortfalls and the cost of grid electricity purchases low. We then examine the computational and memory requirements of the aforementioned prediction and optimization algorithms and find that they are within the capabilities of modern embedded system microprocessors and, hence, are amenable for deployment in typical households and communities.**

***Index Terms*—Cyber-Physical System (CPS), distributed embedded system, energy management system, optimization, sensor networks, Smart Grid.**

I. Introduction

THERE HAS been significant interest in Cyber-Physical Systems (CPSs) in recent years [1]. CPS refers to systems which have a tight coupling between the digital and physical worlds and comprises sensors which measure, and actuators which affect, processes in the physical world, together with the necessary computational and networking architecture and information processing algorithms. Although CPS was initially of interest in the defense and security domains, it is increasingly viewed that CPS can play an important role in civilian and commercial domains, especially in a world grappling with climate change and concerned about improving sustainability and efficiency in a wide range of activities. Examples are energy management at the household, community, and regional levels and congestion management in transportation systems.

In order to reduce the production of greenhouse gases from traditional power-generation plants, there is increasing interest in generating electric power from renewable-energy sources such as solar and wind. Frequently, these renewable-energy sources need to be integrated with and supplement the main electricity grid. However, the power output from renewable-energy sources are affected by dynamic environmental conditions such as the changing intensity of sunlight and wind speed.

The Smart Grid with enhanced communication and sensing capabilities [2] enables closer real-time interaction between energy producers and users, e.g., through the Advanced Metering Infrastructure (AMI), and facilitates the control and integration of renewable-energy sources to the main grid. These capabilities go beyond those of the existing Supervisory Control and Data Acquisition (SCADA) systems presently employed for distribution automation and in distribution management systems. In the area of sensing, we distinguish between sensing for control, e.g., the status of various power systems equipment and the power flows between them, and *ambient sensing*, with the latter, typically in the form of wired and wireless sensor networks which sense various environmental phenomena, being the focus of this paper.

Related to the Smart Grid, demand response schemes, in which users are given incentives to reduce their energy use during peak periods, are being considered by utility companies. The rationale behind demand response is that the production of energy to meet the peak demand either exceeds the available generation or transmission capacity, or the costs, both monetary as well as in terms of impact on the environment, of producing this higher amount of energy would be significantly higher since the generating equipment would need to operate outside their efficient operating regions.

Demand response schemes have had limited success so far [3]. This is mainly due to the difficulty in tailoring static incentives or tariffs to achieve the desired level of energy consumption from users whose energy demands are different and affected by many factors, and which are also variable over time. Charging users dynamic real-time prices in a fair manner would be an enhancement over the static schemes.

Understanding the underlying causes behind user demand would enable better design of demand response schemes. This

Manuscript received February 5, 2012; revised July 3, 2012; accepted August 25, 2012. Date of publication February 7, 2013; date of current version June 12, 2013. This work was supported by the EDASACEP project of the A*STAR Singapore SERC DVCaaS TSRP research programme. This paper was recommended by Associate Editor A. Konar.

C.-K. Tham is with the Department of Electrical and Computer Engineering, National University of Singapore, Singapore 119260 (e-mail: eletck@nus.edu.sg).

T. Luo was with the Department of Electrical and Computer Engineering, National University of Singapore, Singapore 119260. He is now with the Institute for Infocomm Research, A*STAR, Singapore 138632 (e-mail: luot@i2r.a-star.edu.sg).

Color versions of one or more of the figures in this paper are available online at http://ieeexplore.ieee.org.

Digital Object Identifier 10.1109/TSMCA.2012.2224337

is where information from ambient sensing can make a difference since users' energy demands are not totally random. For example, on a hot day, energy demand is likely to be high since many people will turn on their air conditioners. Furthermore, they are likely to ignore signals to reduce energy consumption under these conditions. Apart from its usefulness for the demand side, ambient sensing can also provide valuable indications from the perspective of the supply side, such as the expected power output from renewable-energy sources under various ambient conditions.

Ambient sensing has been employed in building energy management systems [4], typically to detect the level of occupancy in different areas of the building so that lighting, heating, ventilation, and air conditioning can be turned on at the appropriate level at each area in order to conserve energy. Our focus in this paper is different in that we make use of ambient sensing achieved through a CPS at the household and community levels to predict user demand and electricity supply from renewable sources, and then make decisions on when and how much electricity each household should purchase from the main grid based on these predictions.

The rest of this paper is organized as follows. In Section II, we describe a Smart Grid CPS (SG-CPS) and the functional components within it. In Section III, we describe methods to predict the demand and supply of electricity and formulate prediction-based energy purchasing schemes. In Section IV, we propose optimization-based methods for making energy purchase decisions using linear programming (LP) and multi-stage stochastic programming (SP). Section V evaluates the performance of these methods by examining the costs and shortfalls[1] that occur and the grid purchase quantities. Section VI analyzes the system performance in terms of computation time and memory requirements and assesses the feasibility of running the aforesaid algorithms on an embedded energy management system. Finally, Section VIII presents concluding remarks.

A. Contributions

The contributions of this paper are threefold.

1) Use of ambient sensors in a CPS to enable the real-time prediction of the following: a) electricity output from renewable-energy sources and b) electricity demand in a household or community.[2]
2) Development of an optimization-based grid electricity purchasing decision maker that uses LP or multi stage SP to make decisions with look-ahead which result in a significant reduction in the occurrence of electricity shortfalls while keeping the cost of purchasing electricity from the grid low.
3) Analysis of the computational and memory costs of the prediction and purchasing decision algorithms to evaluate the feasibility of realizing the entire SG-CPS scheme on an embedded energy management system.

Optimization methods using LP and SP have been used by electricity-generation companies to determine electricity-generation schedules [5] and manage energy portfolios [6]. Typically, generation dispatch management and power flow optimization are done on a day-ahead basis based on the data from SCADA systems. In this paper, we consider the case of making real-time electricity purchasing decisions at every time interval, e.g., hourly, using several techniques, including LP and SP, in a home or community setting in which renewable-energy sources and ambient sensing facilities are available.

II. SG-CPS Architecture

The system architecture of the SG-CPS which we have designed and prototyped is shown in Fig. 1. SG-CPS can operate either at the individual household level or at the community level comprising several households.

The objective of SG-CPS is to make decisions on the quantity and timing of grid electricity to purchase, taking into account the power-generation output of renewable-energy sources in the household or community, such as photo-voltaic (PV) cells capturing solar energy and wind turbines (WTs) capturing wind energy, as well as the electricity demands of the household or community.

The price of grid electricity changes in real time as it reflects the demand and supply conditions of the electricity market [7], [8], as well as the costs of generation, e.g., fuel prices, faced by the generating company. The real-time grid electricity prices and purchasing transaction system are accessible by the SG-CPS through a secure Internet connection.

We consider the operating scenario whereby a grid electricity purchasing decision, in terms of the quantity of grid electricity required throughout the duration of a fixed time interval, has to be made at the beginning of the time interval. The cost of the transaction is based on the real-time price of grid electricity when the purchase is made.

There is an energy storage device in the form of a high-capacity battery bank which can supply some amount of energy when there is a temporary shortfall, which happens when the actual electricity demand is greater than the electricity supply from the renewable-energy sources. The energy storage device is also useful for storing energy when there is a surplus.

Since the electricity demand in the household or community and supply from renewable-energy sources throughout the time interval cannot be known in advance, these two quantities need to be predicted at the start of the time interval when the electricity purchasing decision needs to be made. The predictions are made by the demand predictor and supply predictor.

The supply predictor receives real-time sensing data streams from sunlight and windspeed sensors and uses a model of electricity supply from PV and WT renewable-energy sources under different conditions.

As mentioned in Section I, we also use information from ambient sensors, in particular, real-time sensing data streams from temperature and humidity sensors, to predict users' electricity

[1]These shortfalls are not outages as there is no interruption to the user. It simply means that the electricity from renewable-energy sources and storage are not enough to meet the requirements of the user at that moment, and some electricity has to be purchased from the main grid, as is done all the time in conventional electricity grids.

[2]Smart meters in the AMI can measure load in real time but usually do not attempt to predict future load.

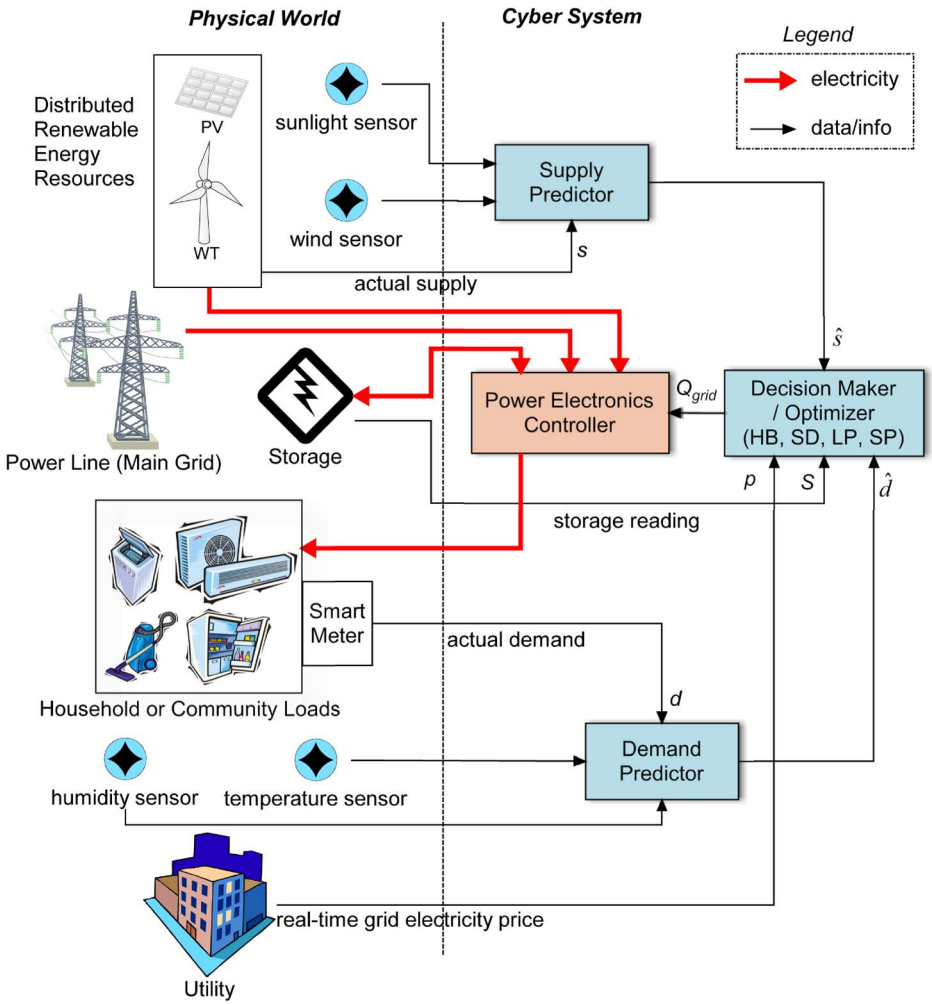

Fig. 1. Architecture of SG-CPS.

demands. The demand and supply predictors will be described in greater detail in Section III.

The predictions of demand and supply based on real-time sensor information and historical data, and the current and historical real-time price of grid electricity are fed into a grid electricity purchasing decision maker that not only tries to satisfy immediate needs but also projects into the near-term as well. This decision maker will be described in greater detail in Section IV. As mentioned above, the grid electricity purchasing decision is made at the start of the time interval and entered directly into the grid electricity purchasing transaction system.

The aforementioned components are implemented in an SG-CPS prototype system (see Fig. 1) with sensing data streams feeding into a computer with MATLAB installed, on which the demand and supply predictors and the grid electricity purchasing decision maker execute to work out the grid electricity purchasing decisions. On the physical world side of the total CPS picture, the computer is connected to a power electronics controller which regulates electrical energy flow between the main electricity grid, renewable-energy sources, storage, and the electrical loads in the household or community. Examples of these loads are household appliances like refrigerators, air conditioners, and heaters. The actual energy consumed by these electrical loads, or the actual demand, can be measured using smart meters. The power electronics controller also contains switches or relays that can either connect the entire household or community, or specific types of loads, to the main grid in the "connected" mode of operation, or isolate them from the main grid in the "islanded" mode of operation.

Our eventual goal is to reduce the system requirements from a computer to an embedded energy management system with a smaller footprint that can be deployed in a cost-effective manner in typical households and communities.

III. Demand and Supply Prediction

We consider the situation in which a decision on the quantity of electricity to purchase from the main grid needs to be made at the start of every time slot, for example, of 1-h duration.

A basic method for a customer to make this decision is to assume that the demand and supply throughout a particular time slot under consideration would be the same as the actual demand and supply throughout the previous time slot. Taking into account the current available storage energy, the customer then purchases the shortfall, if any, from the main grid. This basic method, which we shall refer to as the *baseline* method,

has drawbacks as it does not take into account the volatile demand and supply conditions.

In the following sections, we describe prediction methods for demand and supply which utilize historical information as well as ambient sensing information in order to achieve more accurate predictions. Although there are fairly advanced models for predicting user demand patterns, e.g., [9], and predicting supply from renewables, e.g., [10], [11], we restrict ourselves to relatively simple prediction and energy storage models in our approach since our goal is to execute these models in real time on low-cost embedded energy management systems installed at each household or community.

A. Demand Prediction

A demand or load prediction method is needed as it is unrealistic to assume that users know their future household electricity requirements and can indicate this to the energy management system. First, and in general, users use energy either in reaction to dynamic environmental circumstances or spontaneously out of their own needs or mood. However, users also have habitual usage behaviors which give rise to patterns that can be exploited for demand prediction [12]. Second, most users would find it laborious to estimate their energy consumption and decide on the amount of electricity to purchase in each, e.g., hourly, time slot of the day.

In this section, we describe two prediction methods of user demand which are effective and have low computational requirements. One method is called history-based (HB) prediction, which predicts the demand on day $N+1$ in time slot i to be the average of the actual demand over the previous N days, i.e.,

$$\hat{d}_{\mathrm{HB}}(N+1,i) = \frac{1}{N}\sum_{l=1}^{N} d(l,i). \tag{1}$$

The other method is called sensing-driven SD prediction which, in addition to using historical data, also uses temperature and humidity sensor readings. The rationale is that the demand is affected by weather conditions which can be measured using ambient sensors. The following model can be viewed as a simplified form of the model proposed in [9] which incorporates temperature and humidity to predict household electricity demand.

Denote by $\tilde{t}_p(l,t)$ the sensor reading of room temperature and by $\tilde{h}_u(l,t)$ that of humidity (converted into relative humidity, RH [13]), on day l at time t. Denote the tuple $\langle \tilde{t_p}(l,t), \tilde{h}_u(l,t)\rangle$ by $\mathbf{x}(l,t)$. SD prediction interpolates the demand $\hat{d}_{\mathrm{SD}}(N+1,i)$ based on historical samples $d(l,i)$ and sensor readings $\mathbf{x}(l,t)$ where t is at the start time of slot i, using Shepard's method [14], as follows:

$$\hat{d}_{\mathrm{SD}}(N+1,i) = \sum_{l=1}^{N} \frac{w_l(\mathbf{x})d(l,i)}{\sum_{j=1}^{N} w_j(\mathbf{x})} \tag{2}$$

where $w_l(\cdot)$ is a weighting function with its classic form $w_l(\mathbf{x}) = \|\mathbf{x}-\mathbf{x}_l\|^{-p}$, $\mathbf{x}$ is $\mathbf{x}(N+1,t)$, and $\mathbf{x}_l$ is $\mathbf{x}(l,t)$ for simplicity of notation, $\|\cdot\|$ denotes the Euclidean distance, and $p \in \mathbb{R}^+$ is a power parameter chosen by the user. We do not use this classic form but use a modified form that has been found by Franke and Nielson [15] to give superior results:

$$w_l(\mathbf{x}) = \left[\frac{(R_w - \|\mathbf{x}-\mathbf{x}_l\|)_+}{R_w \cdot \|\mathbf{x}-\mathbf{x}_l\|}\right]^2 \tag{3}$$

where $(\cdot)_+$ is the non-negative operator and R_w is a radius of influence about each sample point, which excludes sample points that are far away from the point of interest $\mathbf{x}$.

B. Prediction of Supply From Renewables

We consider a household or community with renewable-energy sources, e.g., a solar PV system and a WT system, as well as energy storage, e.g., a battery bank. The PV system converts sunlight into electricity, and the WT system converts the kinetic energy of wind into electricity. Energy storage in the form of a battery bank is typically used together with PV and WT systems, and can serve as a secondary electricity supply.

The household uses the PV and WT systems as the primary electricity supply and, when it is not sufficient to meet the demand, resorts to the storage as the secondary supply. If it is still short of supply, the household will purchase electricity from the main grid as the last resort. At any time, if there is a surplus (either from the renewable sources or over-purchase from the main grid), it will be used to charge the storage.

Note that, when electricity prices are low and high demand is expected, the user may also *overbuy* electricity from the grid and store the surplus for future use. This motivates an intelligent energy purchasing scheme that uses demand and supply predictions, which is investigated in this paper.

1) Modeling Renewable-Energy Sources: The power conversion process of a solar PV system can be modeled [16] as

$$P_s = \eta E_s A_s \tag{4}$$

where P_s is the output electric power from the solar PV, η is the energy conversion efficiency, E_s is the sunlight irradiance, and A_s is the total surface area of all the solar cells on the solar panel.

Although there are more advanced models for estimating the power output of a solar PV system, e.g., [10], that include additional factors such as weather condition, PV tilt angle, clock time, date of the year, and ambient temperature (or PV skin temperature), the model based on (4) above captures the most significant factors and is sufficient to give a good approximation of the power output of the solar PV system.

The power conversion process of a WT system can be modeled [17] as

$$P_w = \frac{1}{2}\rho A_w v^3 C_p \tag{5}$$

where P_w is the output electric power from the WT, ρ is the air density, v is the wind speed, C_p is the power coefficient which is subject to the Betz limit of 0.593, and A_w is the swept area of the turbine which can be calculated as $A_w = \pi r^2$ where r is the length of the turbine blades.

Similar to the case for solar PV above, there are more advanced models for estimating the power output of a WT

system, e.g., the model in [11] is more accurate when the wind speed exceeds certain limits. However, the model based on (5) captures the salient factors and is sufficient for our purpose.

Ambient sensing techniques can be used to determine the sunlight irradiance and wind speed, which, together with the PV and WT models above, enable the prediction of the power that can be provided by the renewable-energy sources.

2) Renewable Supply Prediction: Solar and wind sensor readings are captured at the start of each time slot, for example, i, and converted into sunlight irradiance $\tilde{E}_s(i)$ and wind speed $\tilde{v}(i)$ quantities, respectively.

The total power supply from the renewable-energy sources can then be predicted in an SD manner using (4) and (5), as follows:

$$\hat{s}_{\mathrm{SD}}(t) = \frac{1}{2}\rho A_w \tilde{v}^3(i) C_p + \eta \tilde{E}_s(i) A_s. \tag{6}$$

3) Modeling Energy Storage: Next, we model energy storage in a battery bank. The discharging process of a lead-acid battery follows Peukert's law [18]:

$$C_b = I^k \Delta t$$

where C_b is the battery capacity (in A $\cdot$ h), I is the discharge current, Δt is the discharging period (in hours), and k is the Peukert constant which typically ranges between 1.1–1.3. The charging process is determined by both the charging cycle time, denoted by T_c, and charging efficiency, denoted by η_c. Letting $S(t)$ be the residual battery storage at time t, we have $S(t+\Delta t)$, shown at the bottom of the page. In the case of discharging, P_b is the output power from the battery at the operating voltage of the appliances in the residence, i.e., 230 V in the EU and Singapore, or 110 V in the USA. In the case of charging, $S_{\max}$ is the maximum storage of the battery, T_c is the full charging cycle time, $E_c(\Delta t)$ is the charging electrical energy provided during Δt, η_c is the charging efficiency which, commonly taken to be 75%, is the product of net coulomb efficiency and voltage efficiency. The charging case is an approximation because an exact characterization involves various material and environmental factors which lead to a more complicated model. This approximation suffices when Δt is small, such as half- or 1-h periods.

C. Prediction-Based Energy Purchase

Based on the predicted demand and supply, the amount of electricity to purchase from the main grid at the beginning of time slot i can be determined according to the following:

$$Q_{\mathrm{grid}}^{\mathrm{pred}}(i) = \max\left\{0, \hat{d}(i) - \hat{s}_{\mathrm{SD}}(i) - S(i)^{\frac{1}{k}}\right\} \tag{8}$$

where we omit the day index $N+1$ for clarity, $S(i)$ is the storage quantity at the beginning of time slot i (or, equivalently, the end of slot $i-1$), and k is the Peukert constant as in (7), shown at the bottom of the page. Intuitively, this method purchases the amount that the predicted demand exceeds the predicted supply from the renewables and the storage. We shall refer to this as the HB or SD decision method according to whether $\hat{d}(i)$ is taken to be $\hat{d}_{\mathrm{HB}}(i)$ or $\hat{d}_{\mathrm{SD}}(i)$.

While being an improvement over the basic baseline method mentioned earlier, the HB and SD decision methods are still "myopic" as they only look ahead into the future by one time slot. Due to the dynamic nature of real-time grid electricity prices, it may be advantageous to *overbuy* electricity when the price is low and stock the surplus in the energy storage for future use when the price becomes high. Hence, it would be beneficial to design better decision methods that take into account price information and look further ahead into the future. These aspects will be addressed in the next section.

IV. Optimization-Based Purchasing Decision Methods

Our goal is to design a purchasing decision method that minimizes the cost of purchasing electricity from the main grid while also minimizing the occurrence of shortfalls. A shortfall happens when supply from renewable sources and storage plus the purchased amount from the main grid at the start of the time interval is insufficient to meet the actual user demand. Note that a shortfall may arise in the middle of a particular time slot, while the purchasing decision had to be made at the beginning of the time slot. When a shortfall arises, electricity is tapped from the main grid to fulfill the user's demand, i.e., there is no outage, but a penalty in the form of a substantially higher grid electricity price will be imposed for the amount supplied from the main grid to meet the shortfall.

In this section, we describe the design of two optimization-based energy purchasing decision methods. A salient feature in these methods is the use of predictions of demand, supply, and grid electricity prices in future time slots. These predictions are the following.

1) The demand and supply predictions for the current time slot use SD prediction [(2) and (6)] based on current sensor readings.
2) The demand and supply predictions for future time slots use HB prediction [(1) and (9)]:

$$\hat{s}_{\mathrm{HB}}(N+1, i) = \frac{1}{N}\sum_{l=1}^{N} s(l, i). \tag{9}$$

where $s(l, i)$ is the actual supply from renewable-energy sources on day l and time slot i.

$$S(t+\Delta t) = \begin{cases} \max\left\{S(t) - P_b^k \Delta t, 0\right\}, & \text{when discharging,} \\ \min\left\{S_{\max}, S(t) + \min\left\{\frac{S_{\max}}{T_c}\Delta t, \eta_c E_c(\Delta t)\right\}\right\}, & \text{when charging.} \end{cases} \tag{7}$$

3) The price prediction for future time slots will also use HB prediction in a way similar to (1) and (9).

Note that the current grid electricity price is provided by the utility company, as shown in Fig. 1.

The goal mentioned above is formulated into objective functions with constraints that take into account all available information, i.e., physical limits, sensor measurements, historical data, and future predictions. Thereafter, LP and multi-stage SP optimization techniques are used to solve them in order to determine the quantity of grid electricity to purchase at the start of the present time slot. These aspects will be discussed in the remainder of this section. The computational and memory requirements of these decision methods will be examined in Section VI.

A. LP-Based Decision Method

We first derive a purchasing decision method based on LP. In the next section, we shall extend the model to deal with uncertainties in demand and supply predictions.

Given vectors $\hat{\mathbf{d}}$ and $\hat{\mathbf{s}}$ of predictions of demand and supply and assuming that the predictions are accurate, purchasing decisions can be determined by solving the following linear program:

$$\text{minimize} \sum_{i=1}^{T} p(i)Q^{lp}_{\text{grid}}(i) \tag{10}$$

$$\text{s.t. } S(i) + Q^{lp}_{\text{grid}}(i) + \hat{s}(i) \geq \hat{d}(i) + S(i+1) \tag{11}$$

$$S(i+1) - S(i) \leq S_{\max}/T_c \tag{12}$$

$$S(i) \leq S_{\max}$$

$$Q^{lp}_{\text{grid}}(i), S(i) \geq 0, \quad \forall i = 1, 2, \ldots T \tag{13}$$

where i is the index of a time slot (we consider 1-h time slots), T is the look-ahead horizon, $Q^{lp}_{\text{grid}}(i)$ is a decision variable corresponding to the grid purchase quantity at the beginning of period i, and $p(i)$ is the price per kilowatt-hour of electricity from the grid at time slot i. In this model, apart from (12), we assume that battery charging and discharging processes are fully efficient (i.e., Peukert constant $k = 1$ and charging efficiency $\eta_c = 1$); otherwise, the formulation will involve mixed-integer non-LP.

Constraint (11) together with (13) in the above formulation imply that whenever the storage reaches the maximum capacity $S_{\max}$, any energy surplus is dissipated. The constraint (11) and the objective function (10) imply that demand $\hat{d}(i)$ is always satisfied for all i, and moreover, it will always be satisfied by purchasing the minimum amount of $Q^{lp}_{\text{grid}}(i)$. On the other hand, by being prescient on future demand and supply, the model will try to exploit the available storage by purchasing more $Q^{lp}_{\text{grid}}(i)$ whenever the price $p(i)$ is low.

The algorithm is outlined below, which is executed once at the beginning of every time slot.

Algorithm 1 LP-based Decision Method

Input: current (day $N+1$, time slot i, time t_i (start of time slot i)) sensor readings $\tilde{E}_s, \tilde{v}, \tilde{t}_p, \tilde{h}_u$, historical sensor readings of $\tilde{t}_p(l, t_i), \tilde{h}_u(l, t_i)$, historical demands $d(l, i)$, $l = 1, \ldots, N$, and storage $S(i)$

Output: grid purchase quantity $Q^{lp}_{\text{grid}}(i)$

1: compute $\hat{d}(i)$ according to (2)
2: compute $\hat{d}(i+1), \hat{d}(i+2), \ldots, \hat{d}(i+T-1)$ according to (1)
3: compute $\hat{s}(i)$ according to (6)
4: compute $\hat{s}(i+1), \hat{s}(i+2), \ldots, \hat{s}(i+T-1)$ according to (9)
5: run LP solver to solve (10) to determine Q^{lp}_{grid}
6: **return** Q^{lp}_{grid}

B. Multi-Stage SP-Based Decision Method

The LP-based decision method relies on highly accurate predictions of future demand and supply which are difficult to achieve in practice. The effects of inaccurate predictions can be significant: For example, if the actual demand minus supply, $d(i) - s(i)$, is larger than what is predicted, i.e., $\hat{d}(i) - \hat{s}(i)$, and if this persists until the storage runs out, a shortfall will occur.

In order to handle uncertainties arising from the use of predictions, we utilize multi-stage SP [19] which is able to take *posterior recourse* actions to compensate for inaccurate predictions.

For clarity of exposition, variables henceforth will be indexed explicitly by t_i (instead of i) which is the beginning time of time period i. That is, since the actual, i.e., the realization of, demand and supply are only available at the end of period i (or the beginning of period $i+1$), the corresponding variables will be indexed by t_{i+1}, i.e., $d(t_{i+1})$ and $s(t_{i+1})$. Let $\{\mathcal{F}(t_i)\}_{i\geq 1}$ be a filtration generated by past decisions made up to time t_i and past realizations of demand and supply up to time t_i. This means that $Q^{sp}_{\text{grid}}(t_i) \in \mathcal{F}(t_i)$ and $d(t_i), s(t_i) \in \mathcal{F}(t_i)$. At t_i, we make a decision of $Q^{sp}_{\text{grid}}(t_i)$ based on information up to time t_i, that is, $Q^{sp}_{\text{grid}}(t_i)$ is non-anticipatory, and we say that it is adapted to $\mathcal{F}(t_i)$.

We define the disutility experienced by the user at period i as

$$\text{Disutility}(t_i) = p(t_i)Q^{sp}_{\text{grid}}(t_i) + F \cdot p(t_i)\psi(t_{i+1}) \tag{14}$$

where $F > 1$ is a penalty factor and $\psi(t_{i+1})$ is the electricity shortfall that occurred during period i (realized at time t_{i+1}). Here, $\psi(t_{i+1}) \in \mathcal{F}(t_{i+1})$ since it relies on the decision of $Q^{sp}_{\text{grid}}(t_i)$ (at the start of period i) and realization of supply and demand, $s(t_{i+1})$ and $d(t_{i+1})$ (at the end of period i).

Let us first consider a one-period problem for finding $Q^{sp}_{\text{grid}}(t_i)$ at time t_i, i.e., two-stage SP. We modify (11) to $S(t_i) + Q^{sp}_{\text{grid}}(t_i) + \psi(t_{i+1}) + s(t_{i+1}) \geq d(t_{i+1}) + S(t_{i+1})$, and after rearranging, we obtain

$$S(t_i) + Q^{sp}_{\text{grid}}(t_i) + \psi(t_{i+1}) - S(t_{i+1}) \geq X(t_{i+1}) \tag{15}$$

where the storage $S(t_i)$ is known at time t_i, $X(t_{i+1}) \in \mathcal{F}(t_{i+1})$ is a random variable denoting $d(t_{i+1}) - s(t_{i+1})$ (which is unknown at t_i), and $S(t_{i+1})$ and $\psi(t_{i+1})$ are both in $\mathcal{F}(t_{i+1})$. We model $X(t_{i+1})$ as a normally distributed random variable with mean $\mathbb{E}[X(t_{i+1})] = \bar{X}(t_{i+1}) = \hat{d}(t_i) - \hat{s}(t_i)$. Assuming independence between actual demand and actual supply, we also have the variance of $X(t_{i+1})$, which is estimated from historical data, as follows:

$$\text{Var}\left(X(t_{i+1})\right) = \frac{1}{T-1}\sum_{i=t-T}^{t-1}\Bigg[\left(\hat{d}(t_i) - d(t_{i+1})\right)^2 + \left(\hat{s}(t_i) - s(t_{i+1})\right)^2\Bigg]. \quad (16)$$

The two-stage stochastic program for the above model is formulated as

$$\begin{aligned}
\text{minimize } & p(t_i)Q^{sp}_{\text{grid}}(t_i) + F \cdot p(t_i)\mathbb{E}\left[\psi(t_{i+1})\right] \\
\text{s.t. } & S(t_i) + Q^{sp}_{\text{grid}}(t_i) + \psi(t_{i+1}) - S(t_{i+1}) \geq X(t_{i+1}) \\
& S(t_{i+1}) - S(t_i) \leq S_{\max}/T_c \\
& S(t_{i+1}) \leq S_{\max} \\
& Q^{sp}_{\text{grid}}(t_i), S(t_{i+1}), \psi(t_{i+1}) \geq 0. \quad (17)
\end{aligned}$$

If we assume that the random variable $X(t_{i+1})$ is represented by two samples with equal probability: $X(t_{i+1})_1 = X(t_{i+1}) + \delta$ and $X(t_{i+1})_2 = X(t_{i+1}) - \delta$, where δ is chosen such that the samples $X(t_{i+1})_1$ and $X(t_{i+1})_2$ satisfy the above mean and variance requirements, we now have the following formulation:

$$\begin{aligned}
\min\ & p(t_i)Q^{sp}_{\text{grid}}(t_i) + Fp(t_i)\left[\frac{1}{2}\psi(t_{i+1})_1 + \frac{1}{2}\psi(t_{i+1})_2\right] \\
\text{s.t. } & S(t_i) + Q^{sp}_{\text{grid}}(t_i) + \psi(t_{i+1})_1 - S(t_{i+1})_1 \geq X(t_{i+1})_1 \\
& S(t_i) + Q^{sp}_{\text{grid}}(t_i) + \psi(t_{i+1})_2 - S(t_{i+1})_2 \geq X(t_{i+1})_2 \\
& S(t_{i+1})_1 - S(t_i) \leq S_{\max}/T_c \\
& S(t_{i+1})_2 - S(t_i) \leq S_{\max}/T_c \\
& S(t_{i+1})_1, S(t_{i+1})_2 \leq S_{\max} \\
& Q^{sp}_{\text{grid}}(t_i), S(t_{i+1})_1, \psi(t_{i+1})_1, S(t_{i+1})_2, \psi(t_{i+1})_2 \geq 0.
\end{aligned}$$

That is, we have converted the problem into a deterministic linear program by approximating from samples of $X(t_{i+1})$. We can increase the richness of the approximation by adding more samples.

The extension of the two-stage problem above to a multi-stage problem can be performed in a similar way by constructing a *scenario tree*[20]. In this paper, we follow the technique in [21] to construct the scenario tree. An optimization-based decision method to determine the grid electricity purchase quantity that takes into account the uncertainty in prediction can then be determined in the following way:

1) Scenario Tree Construction: The scenario tree is an explicit representation of the randomness in $X(t_i)$ as it evolves through time. Since $X(t_i)$ has non-finite support, we approximate it by discrete samples satisfying the same mean and the same variance.

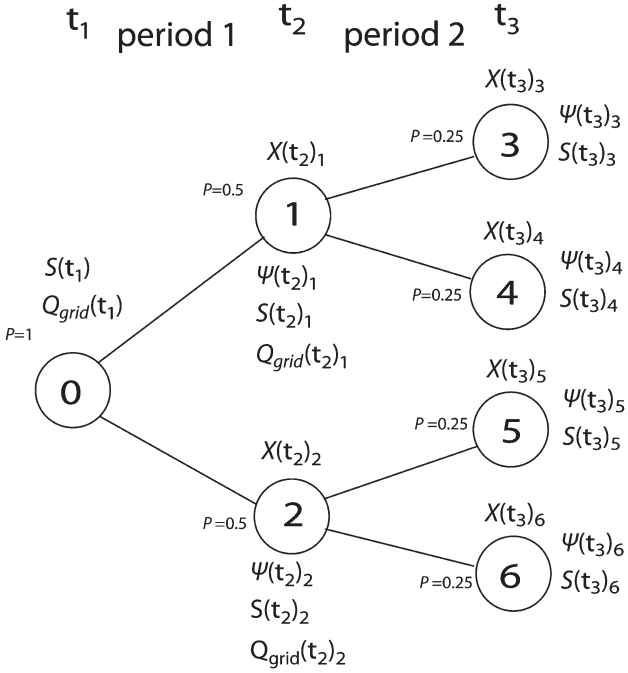

Fig. 2. Example of a two-period scenario tree with each parent having two child nodes.

Fig. 2 shows an example of a typical scenario tree with two child nodes for each parent node. The root node is node 0 which represents the present time t_1. At this node, the information available to the user is the storage $S(t_1)$, the prediction of demand and supply, $\hat{d}(t_1)$ and $\hat{s}(t_1)$. Based on these, the user is to make a decision on $Q_{\text{grid}}(t_1)$. The tree then branches to node 1 and node 2 which represent all the possible realizations of random variable $X(t_2)$: $X(t_2)_1$ and $X(t_2)_2$. At this time instance, depending on the decision made on $Q_{\text{grid}}(t_1)$, the variables $\{\psi(t_2)_1, S(t_2)_1\}$ and $\{\psi(t_2)_2, S(t_2)_2\}$ are revealed, corresponding to the realization $X(t_2)_1$ and $X(t_2)_2$, respectively. This reasoning can be similarly applied to the realizations of $X(t_3)$ at time t_3.

In order to prevent an exponential explosion in the number of scenarios at the end of the look-ahead horizon T, we divide the periods into M segments $\{\phi(k)\}_{k=1,\ldots,M}$ where $1 < M < T$ and the size of each segment are defined by

$$|\phi(k)| = \begin{cases} \left\lfloor \frac{T}{M} \right\rfloor & \text{if } k < M, \\ T - \left\lfloor \frac{T}{M} \right\rfloor (M-1) & \text{if } k = M. \end{cases} \quad (18)$$

where $|\cdot|$ is the number of slots in the segment k. Branching is only performed at the first period of each segment [21]. In our implementation, the number of segments $M = 4$, and the number of branches in each segment is 4.

2) Deterministic Linear Program: Having defined the scenario tree, we are now ready to formulate a linear program to find the best policy. Let n index all the nodes in the scenario tree such that $n = 0$ is the root node. Let $a(n)$ be the index of the parent node of node n, $\mathcal{P}(n)$ be the probability associated with that node, and L be the set of all leaf nodes of the scenario tree. For example, in Fig. 2, we have $a(5) = 2$, $\mathcal{P}(5) = 0.25$,

and $L = \{3, 4, 5, 6\}$. Since each node is distinct, we index the previous variables using n in the new formulation.

Thus, the resultant linear program is formulated as follows:

$$\begin{aligned}
\min \ & \sum_{\forall n \notin L} \mathcal{P}(n) p(n) Q^{sp}_{\text{grid}}(n) + F \sum_{\forall n \neq 0} \mathcal{P}(n) p\left(a(n)\right) \psi(n) \\
\text{s.t. } & S\left(a(n)\right) + Q^{sp}_{\text{grid}}\left(a(n)\right) + \psi(n) - S(n) \geq X(n), \forall n \neq 0 \\
& S(n) - S\left(a(n)\right) \leq S_{\max}/T_c, \forall n \neq 0 \\
& S(n) \leq S_{\max}, \forall n \neq 0 \\
& S(n), \psi(n) \geq 0, \forall n \neq 0 \\
& Q^{sp}_{\text{grid}}(n) \geq 0, \forall n \notin L. \qquad (19)
\end{aligned}$$

Intuitively, this SP-based decision method takes into account possible *consequences* of the decision made at each slot and, via the programming, is able to take recourse actions to compensate for inaccuracy in predictions. The corresponding algorithm is outlined below.

Algorithm 2 SP-based Decision Method

Input: same as Algorithm 1
Output: grid purchase quantity $Q^{sp}_{\text{grid}}(i)$

1: same as Algorithm 1 lines 1–4
2: construct scenario tree according to Section IV-B1
3: run the LP solver to solve the converted linear program of (19) to determine Q^{sp}_{grid}
4: **return** Q^{sp}_{grid}

V. Evaluation of Purchasing Decision Methods

We have developed the SG-CPS prototype system (shown in Fig. 1 in Section II), in which the "cyber" side comprises a computer with MATLAB at the core on which user demand and renewable-energy supply predictions and purchasing decision computations are done. This computer receives sensor feeds from a variety of sensors and actuates a power electronics controller. The parameters of the models used for demand and supply prediction can be found in the Appendix.

Using this platform, we evaluate the performance of five purchasing decision methods:

1) HB and SD: prediction-based, i.e., (8) taking $\hat{d}_{\text{HB}}(i)$ and $\hat{d}_{\text{SD}}(i)$, respectively, for $\hat{d}(i)$.
2) LP and SP: optimization-based, i.e., LP and SP, methods described in Section IV.
3) baseline: the basic method mentioned in Section III, which adopts the following formula:

$$Q^{\text{base}}_{\text{grid}}(t) = \max\left\{0, d(t-1) - s(t-1) - S(t)^{\frac{1}{k}}\right\}. \qquad (20)$$

A. Evaluation Results

The performance metrics are the following: *cost* of purchase, *shortfall*, and *disutility* ((14)). For disutility, the penalty factor F (chosen as 2.0 here) together with $p(i)$ reflects the *surcharge* for instantaneous electricity purchase from the main grid to cope with a shortfall.

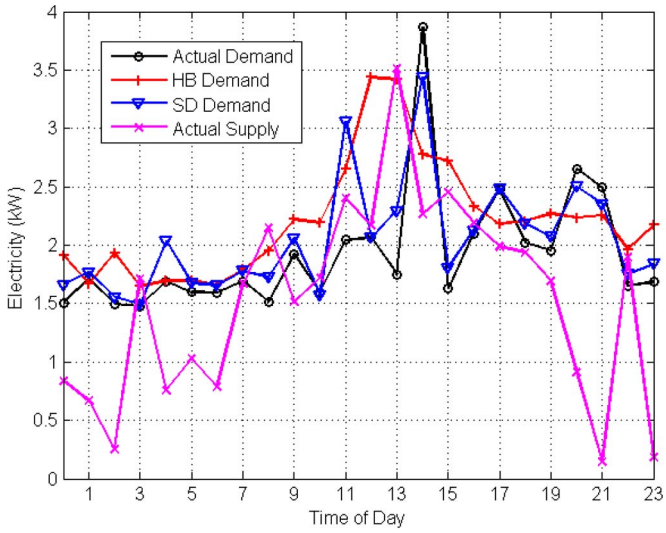

Fig. 3. Demand prediction on a single day.

Before investigating the performance of all the methods, we compare the accuracy of the HB and SD prediction methods for user demand prediction (see Fig. 3). We see that SD prediction follows the actual demand closely while HB prediction is less accurate. The estimation errors for the two predictors are computed by

$$\delta = \frac{1}{24} \sum_{t=1}^{24} \left| \hat{d}(t) - d(t) \right| / d(t) \times 100\%$$

and we obtain $\delta_{\text{HB}} = 24.01\%$ and $\delta_{\text{SD}} = 9.26\%$, i.e., the SD predictor is significantly better. Henceforth, the LP and SP decision methods will use the SD predictor whenever possible, i.e., when ambient sensor readings are available.

Next, we examine the performance of all the purchasing decision methods in terms of the three metrics mentioned above. Fig. 4 shows a clear decreasing trend of disutility as we move from the baseline toward the HB, SD, LP, and SP methods. The HB and SD methods achieve lower disutility than the baseline method by taking advantage of historical information (for demand prediction in HB) and sensor readings (for supply prediction in both HB and SD, and demand prediction in SD) to make more informed purchasing decisions. SD outperforms HB due to its additional use of sensor readings in demand prediction.

However, these two decision methods are still "myopic" as explained in Section III-C. This is improved by the two optimization-based decision methods, LP and SP, which look ahead into future time slots. A look-ahead horizon of $T = 24$ h was adopted. We see that the disutility is further reduced, and the shortfall is substantially less than HB and SD, while the cost is only marginally higher. Their performance benefits come from overbuying electricity when the price is low and using electricity from storage when the price is high. The shortfall of LP and SP is not zero because prediction inaccuracy is unavoidable, and the nonlinear battery model could not be captured in the LP formulation, and an approximation had to

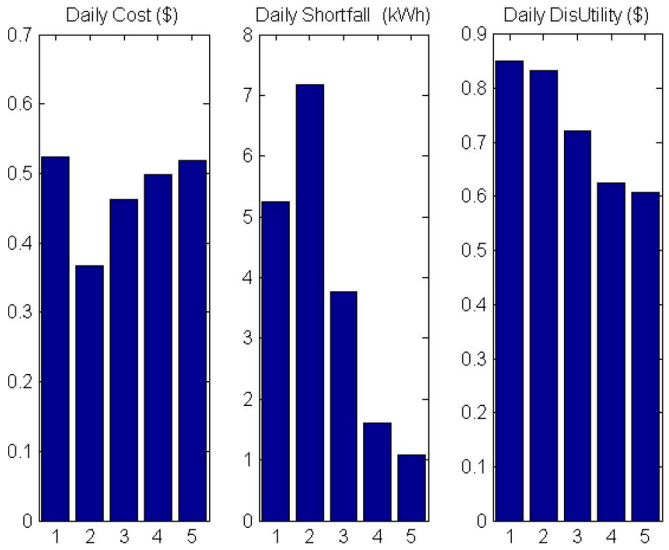

Fig. 4. Performance comparison of cost, shortfall, and disutility (decision methods 1–5 are baseline, HB, SD, LP, and SP).

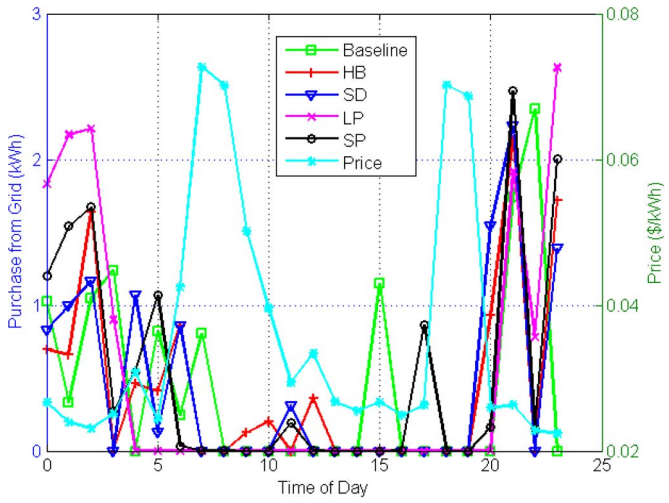

Fig. 5. Grid purchase on a single day.

be used. Since there is prediction inaccuracy, SP outperforms LP because SP has a higher tolerance of inaccuracy than LP, as detailed in Section IV-B.

Then, in Figs. 5 and 6, we examine the hourly purchasing decisions of grid electricity and the storage variation on the same day as that in Fig. 3. The hourly electricity prices shown in Fig. 5 are based on Ameren Illinois [8] since the Singapore EMC real-time prices [7] are applicable only to industrial and commercial customers and not to households and communities. Generally, a good decision method buys more when the price is low and buys less when the price is high. Fig. 5 shows a few instances when this happens. At 7 A.M., when the price is highest for the day, all the schemes do not buy anything from the grid, except baseline. At 11 P.M., when the price is lowest, baseline does not take the opportunity to buy, but all the other decision methods buy large amounts, with LP and SP buying more than HB and SD. Another trend which is exhibited in the storage (Fig. 6) is that LP and SP maintain a higher level of storage than the other schemes. This is because LP and SP buy

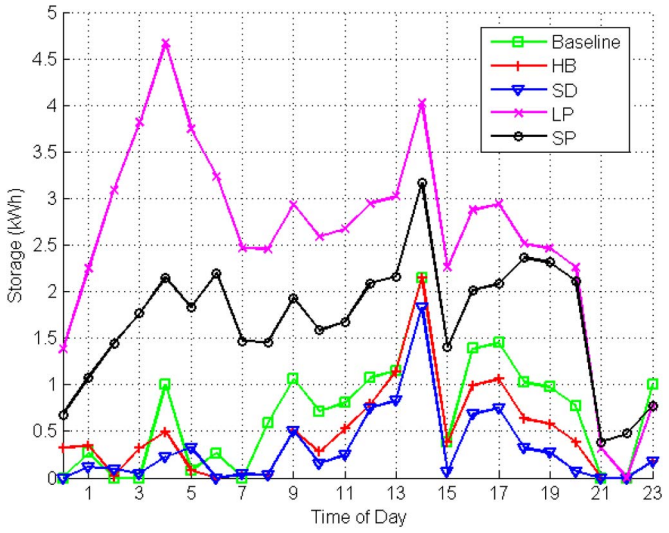

Fig. 6. Storage on a single day.

substantial amounts of electricity in the early hours of the day (starting from late night of the previous day) when the price is at its lowest, which leads to continuous battery charging from 0 to 4 A.M., as can be seen in the figure.

VI. Evaluation of System Performance

In this section, we evaluate the computational complexity of the methods discussed in the earlier sections of this paper, in terms of execution time and memory requirements.

For the LP and SP decision methods, the major computationally intensive aspect lies in the need to solve the LP problem. There have been substantial research efforts to characterize the complexity of solving LP problems. This question had remained open for many years until Khachiyan [22], [23] showed that LP is in the class $\wp$; that is, it can be solved in polynomial time relative to the length of the binary encoding of the input. However, it is still an open question whether a system of linear inequalities can be solved in a number of arithmetic operations that is polynomially bounded by the dimensions of the system. So far, only partial results are known, such as Tardos [24], [25]. Theoretical research in recent years had focused on the asymptotic worst-case complexity of a problem in $\wp$, until a breakthrough result was obtained in [27], namely, for any fixed n, LP problems with n variables and m constraints can be solved in $O(m)$ time as m tends to infinity.

While these theoretical results are useful for deriving performance bounds, practitioners often require definite results and are more interested in the actual execution time or its distribution. In addition, practitioners are concerned with memory requirements. In this paper, we take a practical approach and investigate both time and space complexity of the methods presented in Sections III and IV on our prototype system. We then generalize the results to evaluate the feasibility of implementing these methods on a modern embedded system platform.

To measure the execution time, we use CPU time rather than wall-clock time since the latter is highly dependent on the computing environment such as the operating system and

TABLE I
COMPLEXITY IN TERMS OF CPU TIME AND FLOPS

Method	Intel Core2	FLOPs	ARM Cortex-A8
Baseline	26 ms	0.66 G	0.33 s
HB	29 ms	0.73 G	0.37 s
SD	33 ms	0.83 G	0.42 s
LP	0.229 s	5.79 G	2.89 s
SP	0.652 s	16.48 G	8.24 s

coexisting applications. In order to cater to different CPU models, we convert the measured CPU time into floating-point operations (FLOPs). For illustration purposes, we extrapolate the results to a high-end embedded system based on the ARM Cortex-A8 [28], which is a processor widely used in mildly processing-intensive domains such as smartphones and home networking.

The computer in the prototype SG-CPS system is based on an Intel Core2 Duo processor E8500 with a clock speed of 3.16 GHz and a computational power of 25.28 giga-FLOPs per second (GFLOPS) (note the difference between FLOPS and FLOPs: The capital "S" indicates "per second"). The ARM Cortex-A8 has a clock speed of 0.6–1 GHz and is integrated with a floating point (FP) unit of a VFPv3 architecture [29] which provides 1.3 (VFP9-S) or 2.0 (VFP10) mega-FLOPS/MHz. This translates to a computational power of 0.78–2 GFLOPS. Hence, we are able to compute the expected execution time on the ARM Cortex-A8 based on these specifications and the measured CPU time on the SG-CPS computer.[3]

Measurements of CPU time and memory usage that are presented below were obtained using the MATLAB profiler.

A. Execution Time

For each of the five decision methods, we obtained the execution time by averaging over 336 runs (14 days $\times$ 24 h) and summarized the results in Table I.[4] We can see that the computational cost is low for the baseline, HB, and SD methods, while the cost for LP is significantly higher and the cost for SP is about 3 times that of LP. The bulk of the processing time for the SP method is spent in computing step 3 of Algorithm 2. This points to a tradeoff between the performance of the different decision methods in terms of grid electricity purchasing and shortage costs (described in Section V) versus the computational cost.

Another salient point worth noting is that while these measurements are based on a MATLAB implementation,[5] the final actual deployment on an embedded system will use a compiled form of programs written with an efficient native embedded system language such as C. Furthermore, there are several more mature and efficient LP solvers than the `linprog` function in MATLAB. Therefore, while the execution times shown above are representative, there is still room for improvement in the final deployment.

Moreover, there are more advanced low power ARM processors such as the ARM Cortex-A15 MPCore processor [31] which comes with 1.5–2.5-GHz quad-core configurations and VFPv4 FP support that can deliver several times the performance of the ARM Cortex-A8, which itself has already been superseded by the ARM Cortex-A9 in some devices.

TABLE II
COMPLEXITY IN TERMS OF PEAK MEMORY USAGE

Method	Number of FP no.s	Memory usage (`double` data type)
Baseline	1,325	10.6 kB
HB	4,012	32.1 kB
SD	5,901	47.2 kB
LP	7,812	62.5 kB
SP	2,927,200	23.4 MB

B. Memory Requirements

We also measure the memory consumption over 336 runs using the MATLAB profiler.[6] Instead of taking the average memory usage, we took the *peak* memory usage which is more meaningful. The results for the five decision methods are shown in Table II in terms of the number of FP numbers and the memory usage in the case where the double precision 8-byte `double` data type is used to represent FP numbers (as in the case of MATLAB), including all auxiliary and temporary variables.

Other than SP, all the methods consume only a modest amount of memory. Even the SP method is within the capabilities of most modern embedded systems that are implementable in smart home settings. The memory usage of SP is prominent because its internally used scenario tree (see Section IV-B1) grows exponentially, which results in a much larger linear program than the LP method.

Further code and memory optimizations are possible that would reduce the memory requirements of the five decision methods from the figures shown above. In addition, it is possible to represent FP numbers using the single precision 4-byte `float` data type. In most cases, this should only result in a slight degradation in the quality of the LP solutions.

VII. DISCUSSION

Although the work in [12] discovered persistent daily routines and patterns of consumption or baselines typical of specific weather and daily conditions which explain approximately 80% of household electricity use, there is still a fairly high degree of variability in user electricity demand, as well as in the supply from renewable-energy sources, which makes it difficult to model and predict their values accurately, even

[3]MATLAB had a `flops` command to readily count the FLOPs of a program, but this was discontinued after version 5 and replaced by commands such as `tic/toc` and `cputime`. While some researchers have developed Matlab routines for counting FLOPs, these routines do not work with the `linprog` function, which is the major component in the LP and SP decision methods.

[4]The execution time for ARM Cortex-A8 is given for the faster 2.0 GFLOPS version.

[5]MATLAB programs can be sped up by implementing functions in another language like C, compiling it with `mex`, and then calling that code from within the MATLAB program. The `linprog` function shipped with MATLAB would have been optimized in a similar manner already.

[6]Profiling memory usage was done through an undocumented MATLAB feature described in [32]. The MATLAB profiler gives results in bits, and MATLAB uses the 8-byte `double` data type to represent an FP number.

with advanced methods [9]. Hence, the approach taken in this paper is to use simple prediction methods based on historical and real-time sensor data, coupled with optimization methods that can handle uncertainty, i.e., multi-stage SP. The SP-based decision method takes into account possible consequences of the decision made at each slot and is able to take posterior recourse actions to compensate for inaccuracy in predictions.

In the approach taken in this paper, there are two components: 1) modeling and prediction of user demand and supply from renewables and 2) optimization to determine the energy purchase quantity from the main grid. Modeling techniques such as Markov predictor [33] and Dynamic Bayesian Network the [34] have been shown to work well in other contexts and may be effective for the task considered in this paper. However, these techniques do not address the optimization aspect. One approach can be to combine these modeling techniques with the Markov Decision Process [35] technique for control and optimization. Unfortunately, these techniques are computationally expensive and may take a long time to converge to the optimal solution.

Hill climbing is a local search approach that makes incremental improvements to a starting solution to try to reach the optimal solution. This technique requires significantly less computation compared to LP [37]. However, hill-climbing approaches are often trapped in local optima and are not guaranteed to produce the globally optimal solution. Stochastic hill climbing makes random incremental changes to a starting solution and can sometimes avoid local optima, but, nevertheless, also cannot guarantee finding the global optimum.

On the other hand, the LP and SP methods proposed in this paper guarantee the finding of the optimal solution that satisfies the constraints within a finite amount of time.

VIII. Conclusion

In this paper, we have presented an SG-CPS which enables ambient sensor readings of temperature, humidity, sunlight irradiance, and wind velocity to be used to produce predictions of user demand and supply from renewable sources. These predictions are utilized in a decision making module that has four decision methods which determine the quantity of grid electricity to purchase at each time slot of the day to meet the electrical energy demanded by household and community appliances in a cost-effective manner, while minimizing shortfalls that would require the purchase of electricity at a significantly higher price.

The four decision methods range from fairly simple ones that use demand and supply predictions with limited look-ahead restricted to the current time slot, to two other more sophisticated ones that employ a longer look-ahead horizon and formulate the grid electricity purchasing decisions as optimization problems that are solved using LP or multi-stage SP techniques. Although the latter two methods result in a significant reduction in the occurrence of shortfalls while keeping the cost of purchasing electricity from the grid low, mainly by being able to judiciously purchase and store energy ahead of time, their decision algorithms are more computationally intensive.

By carefully measuring their computation times and memory requirements on the SG-CPS platform and extrapolating them to the capabilities of modern microprocessors used in embedded systems, we conclude that it is feasible to implement the prediction and purchasing decision methods proposed in this paper on small footprint embedded energy management systems that can be deployed in a cost-effective manner in typical households and communities.

One possible alternative approach compared to that adopted in this paper is to use more advanced prediction and modeling methods, such as those mentioned in Section VII and in [9] and [12], together with simpler optimization methods. We leave the study and evaluation of this approach for future work.

Appendix

A. Model Parameters

Typical solar panels today achieve an energy conversion efficiency η of 10%–15% [37] or 5%–18% [38]. For the PV system under consideration, $\eta = 12\%$. The total cell surface area of the solar panel is $A_s = 20$ m^2, and the sunlight irradiance $\tilde{E}_s(t)$ ranges from 0 to 990 W/m^2 corresponding to nocturnal and diurnal times.

For the WT system, air density $\rho = 1.23$ kg/m^3, turbine blade length $r = 10$ m, power coefficient $C_p = 0.4$, and wind speed $\tilde{v}(t)$ can vary between 1 and 3 m/s.

For the battery bank, maximum storage $S_{\max} = 5$ kWh, charging cycle $T_c = 2.5$ h, and Peukert constant $k = 1.2$.

For SD demand prediction, the radius of influence $R_w = 16.4924$.

Acknowledgment

The authors would like to thank G. A. Hanasusanto for his contribution in the formulation of the LP and SP methods.

References

[1] "Program solicitation on Cyber-Physical Systems (CPS)," Arlington, VA, Document NSF 11-516, 2011.
[2] C. H. Hauser, D. E. Bakken, and A. Bose, "A failure to communicate: Next-generation communication requirements, technologies and architecture for the electric power grid," *IEEE Power Energy Mag.*, vol. 3, no. 2, pp. 47–55, Mar./Apr. 2005.
[3] S. K. Vuppala, K. Padmanabh, S. K. Bose, and S. Paul, "Incorporating fairness within demand response programs in Smart Grid," in *Proc. IEEE PES ISGT*, Jan. 2011, pp. 1–9.
[4] V. L. Erickson, Y. Lin, A. Kamthe, and R. Brahme, "Energy efficient building environment control strategies using real-time occupancy measurements," in *Proc. BuildSys*, Berkeley, CA, 2009, pp. 19–24.
[5] X. Peng and P. Jirutitijaroen, "Stochastic unit commitment using multi-cut decomposition algorithm with partial aggregation," in *Proc. IEEE Power Eng. Soc. Gen. Meet.*, San Diego, CA, Jul. 2011, pp. 1–8.
[6] O. Kittithreerapronchai, P. Jirutitijaroen, S. Kim, and J. Prina, "Optimizing natural gas supply and energy portfolios of a generation company," in *Proc. IEEE 11th Int. Conf. Probability Methods Appl. Power Syst.*, Singapore, Jun. 2010, pp. 231–237.
[7] Energy Market Company Pte Ltd (EMC), *Real-Time Prices and Demand*, Singapore. [Online]. Available: http://www.emcsg.com/
[8] "Ameren Illinois rate zone 1, real-time price," St. Louis, MO, 2012.
[9] M. Beccali, M. Cellura, V. L. Brano, and A. Marvuglia, "Short-term prediction of household electricity consumption: Assessing weather sensitivity in a Mediterranean area," *Renew. Sustain. Energy Rev.*, vol. 12, no. 8, pp. 2040–2065, Oct. 2008.

[10] H. Ge, L. Ni, and S. Asgarpoor, "Reliability-based stand-alone photovoltaic system sizing design—A case study," in *Proc. 10th Int. Conf. Probability Methods Appl. Power Syst.*, 2008, pp. 280–287.
[11] C. Novoa and T. Jin, "Reliability centered planning for distributed generation considering wind power volatility," *Elect. Power Syst. Res.*, vol. 81, no. 8, pp. 1654–1661, Aug. 2011.
[12] J. Abreu, F. Pereira, and P. Ferrao, "Using pattern recognition to identify habitual behavior in residential electricity consumption," *Energy Build.*, vol. 49, pp. 479–487, Mar. 2012.
[13] S. Horstmeyer, "Relative humidity," WKRC TV, Cincinnati, OH, 2008.
[14] D. Shepard, "A two-dimensional interpolation function for irregularly-spaced data," in *Proc. ACM Nat. Conf.*, 1968, pp. 517–524.
[15] R. Franke and G. Nielson, "Smooth interpolation of large sets of scattered data," *Int. J. Numer. Methods Eng.*, vol. 15, no. 11, pp. 1691–1704, Nov. 1980.
[16] Wikipedia, Solar Cell Efficiency. [Online]. Available: http://en.wikipedia.org/wiki/Solar_cell_efficiency
[17] F. D. Bianchi, H. de Barrista, and R. J. Mantz, *Wind Turbine Control Systems*. New York: Springer-Verlag, 2007, ch. 2.
[18] M. G. Cugnet, M. Dubarry, and B. Y. Liaw, "Peukert's law of a lead-acid battery simulated by a mathematical model," *ECS Trans.*, vol. 25, no. 35, pp. 223–233, Apr. 2010.
[19] A. Shapiro, D. Dentcheva, and A. Ruszczyski, *Lectures on Stochastic Programming: Modeling and Theory*. Philadelphia, PA: MPS/SIAM, 2009, ser. MPS/SIAM Series on Optimization, ch. 9.
[20] B. Defourny, D. Ernst, and L. Wehenkel, "Multistage stochastic programming: A scenario tree based approach to planning under uncertainty," in *Decision Theory Models for Applications in Artificial Intelligence: Concepts and Solutions*. Hershey, PA: IGI Global, 2011.
[21] M. K. Zanjani, M. Nourelfath, and D. Ait-Kadi, "A multi-stage stochastic programming approach for production planning with uncertainty in the quality of raw materials and demand," *Int. J. Prod. Res.*, vol. 48, no. 16, pp. 4701–4723, Aug. 2010.
[22] L. G. Khachiyan, "A polynomial algorithm in linear programming," *Soviet Math. Dokl.*, vol. 20, pp. 191–194, 1979.
[23] L. G. Khachiyan, "Polynomial algorithms in linear programming," *USSR Comput. Math. Math. Phys.*, vol. 20, no. 1, pp. 53–72, 1980.
[24] E. Tardos, "A strongly polynomial minimum cost circulation algorithm," Inst. Econom. Oper. Res., Univ. Bonn, Bonn, Germany, Rep. No. 84356-OR, 1984.
[25] E. Tardos, "A strongly polynomial minimum cost circulation algorithm," *J. Combinatorica*, vol. 5, no. 3, pp. 247–255, 1985.
[26] E. Tardos, "A strongly polynomial algorithm to solve combinatorial linear problems," Inst. Econom. Oper. Res., Univ. Bonn, Bonn, Germany, Rep. No. 84360-OR, 1985.
[27] N. Megiddo, "Linear programming in linear time when the dimension is fixed," *J. Assoc. Comput. Mach.*, vol. 31, no. 1, pp. 114–127, Jan. 1984.
[28] ARM Cortex-A8 Processor. [Online]. Available: http://www.arm.com/products/processors/cortex-a/cortex-a8.php
[29] *ARM Floating Point Architecture*. [Online]. Available: http://www.arm.com/products/processors/technologies/vector-floating-point.php
[30] *MATLAB R2011b Profiler*. [Online]. Available: http://www.mathworks.com/help/techdoc/ref/profile.html
[31] *ARM Cortex-A15 Processor*. [Online]. Available: http://www.arm.com/products/processors/cortex-a/cortex-a15.php
[32] *Undocumented Profiler Options*, Created: April 2nd, 2009. Addendum: Jan. 31, 2011. [Online]. Available: http://undocumentedmatlab.com/blog/undocumented-profiler-options
[33] Y. Yuan, L. Huang, Y. Tang, D.-J. Deng, and D.-C. Huang, "Improved Markov predictor in wireless networks," *IET Commun.*, vol. 5, no. 13, pp. 1823–1828, Sep. 2011.
[34] K. P. Murphy, Dynamic Bayesian Networks. [Online]. Available: www.cs.ubc.ca/~murphyk/Papers/dbnchapter.pdf
[35] M. L. Puterman, *Markov Decision Processes: Discrete Stochastic Dynamic Programming*. Hoboken, NJ: Wiley, 2005, ser. Wiley Series in Probability and Statistics.
[36] M. Zaharia and S. Keshav, "Fast and optimal scheduling over multiple network interfaces," Univ. Waterloo, Ontario, Canada, Tech. Rep. CS-2007-36, Oct. 2007.
[37] Rainbow Power Company, Sustainable Energy Systems: Photovoltaic Module, New South Wales, Australia. [Online]. Available: http://www.rpc.com.au/products/panels
[38] Wikipedia, Solar Panel. [Online]. Available: http://en.wikipedia.org/wiki/Solar_panel

Chen-Khong Tham (M'91) received the Ph.D. and M.A. degrees in electrical and information sciences engineering from the University of Cambridge, Cambridge, U.K.

From 2006 to 2009, he was the Program Manager of a multi-institution research program on UWB-enabled Sentient Computing (UWB-SC) funded by A*STAR Singapore. From 2007 to 2010, he was on secondment at A∗STAR Institute for Infocomm Research (I2R) Singapore and served as Principal Scientist and Department Head of the Networking Protocols Department, and Program Manager of the Personalization, Optimization & Intelligence through Services (POISe) (Services) Programme. He was an Edward Clarence Dyason Universitas 21 Fellow at the University of Melbourne, Melbourne, Australia. He is an Associate Professor with the Department of Electrical and Computer Engineering, National University of Singapore, Singapore. His current research focuses on sensor network infrastructures and real-time sensor data analytics involving Cyber-Physical Systems, wireless sensor networks, cloud computing, and participatory sensing.

Prof. Tham is in the Editorial Board of the *International Journal of Network Management*, was the General Chair of the IEEE Advanced Information Networking and Applications 2011 and IEEE Asia-Pacific Services Computing Conference 2009 conferences, and was the Organizing Chair of IEEE International Conference on Communication Systems 2012. He and his co-authors were the recipients of the Best Paper award at IEEE International Conference on Ultra-Wideband 2008 and ACM International Conference on Modeling, Analysis and Simulation of Wireless and Mobile Systems 2007.

Tie Luo received the Ph.D. degree in electrical and computer engineering from the National University of Singapore (NUS), Singapore.

He was a postdoctoral Research Fellow with the Computer Networks and Distributed Systems Laboratory, NUS, from 2008 to 2010, and with the Communications & Networks Laboratory, NUS, from 2011 to March 2012. He is currently a Scientist with the Institute for Infocomm Research (I2R), Singapore. His current research interests are participatory sensing, wireless sensor networks, software-defined networking, and OpenFlow.